

S.1 In vitro experiments

S.1.1 Methods

In vitro experiments were performed as a previous step to the in vivo experiments to obtain a first characterization and range of values of the dependence of IRE efficacy on the frequency of the biphasic waveform applied. Monophasic pulses were also used for comparison. Some other studies provided a wide range of lethal EF thresholds in cardiac and non-cardiac cells for different waveforms⁴⁸⁻⁵⁰

CHO cells were grown in complete cell culture medium which consisted of Dulbecco's Modified Eagle Medium (DMEM) with addition of 10% fetal bovine serum and supplemented by antibiotics (100 U/ml penicillin, and 100 µg/ml streptomycin). The cells were maintained in a humidified atmosphere at 37 °C and 5% CO₂ and routinely passed every two days.

On the day of the experiment and after trypsinization, cells were centrifuged for 5 min and resuspended at a density of 1.2×10^6 cells/ml in a low conductivity buffer (LCB) to minimize electrolysis and thermal damage. LCB consisted of 250 mM Sucrose, 10 mM glucose, 10 mM NaCl, 5 mM KCl, 2 mM MgCl₂, 10 mM HEPES, 1.8 mM CaCl₂ (pH: 7.17, conductivity: 2.5 mS/cm, osmolarity: 305 mOsm). Cells suspended in LCB were exposed to electroporation EFs in conventional 1 mm cuvettes. After the delivery of the EF, cells were kept in the cuvettes for 10 min at room temperature. They were then sequentially diluted in complete medium and seeded in technical triplicates at 150 cells per cell culture well (of a 12-well culture plate) to measure their viability through a quantitative cloning efficacy test. After 5 days maintained in a humidified atmosphere, colonies were washed with PBS and fixed/stained with a crystal violet solution (0.2% Crystal Violet, 10% formaldehyde and 20% ethanol in H₂O). The number of clones N for each condition was counted. Viability was normalized to the number of clones in the control (N_{control}) and reported as a percentage of survival: $N/N_{\text{control}} \times 100$. The cells in the controls were handled exactly the same way than the exposed cells including incubation times in cuvettes and dilutions. All the experiments were repeated at least three independent times in at least two different days.

The results of cell survival as a function of EF intensity were characterized with a mathematical probabilistic model⁵¹. In the present study we used a logistic regression as proposed in Perera et al.⁵². Probability of cell survival (P_s) was defined as:

$$P_s(\%) = 100 \frac{1}{(1 + e^{-(\beta_0 + \beta_1 E)})}$$

where, β_0 provides information about the field magnitude at which the transition from living to dead cells occurs and β_1 describes its slope. Matlab 2020a (Mathworks) curve fitting toolbox was

used to fit the data. Finally, for each waveform studied, the EF threshold was derived as the intensity at which 95 % of cells were dead according to the fitted logistic regression.

S.1.2 In vitro cell survival experiments results

In Fig. S1a cell survival results obtained from cloning efficacy experiments and the corresponding fitted logistic regression models are shown for the different conditions studied. As expected, cell survival decreases when the intensity of the EF increases. Furthermore, the EF magnitude necessary to obtain equivalent survival rates considerably increases with frequency. In Fig. S1b the EF thresholds necessary to obtain a 95 % of cell death that were obtained from the logistic models are displayed for each frequency studied. Note that the data corresponding to monophasic pulses is displayed in the low frequency range because square pulses are considered as a quasi-DC waveform. Under these specific experimental conditions, the EF threshold value obtained for monophasic pulses is 1180 V/cm, for biphasic waveforms of 150 kHz is 1412 V/cm, for 250 kHz is 1616 V/cm and for 450 kHz 2024 V/cm. These results show how the EF intensity necessary to obtain an equivalent IRE effect depends non-linearly on the frequency of the waveform applied.

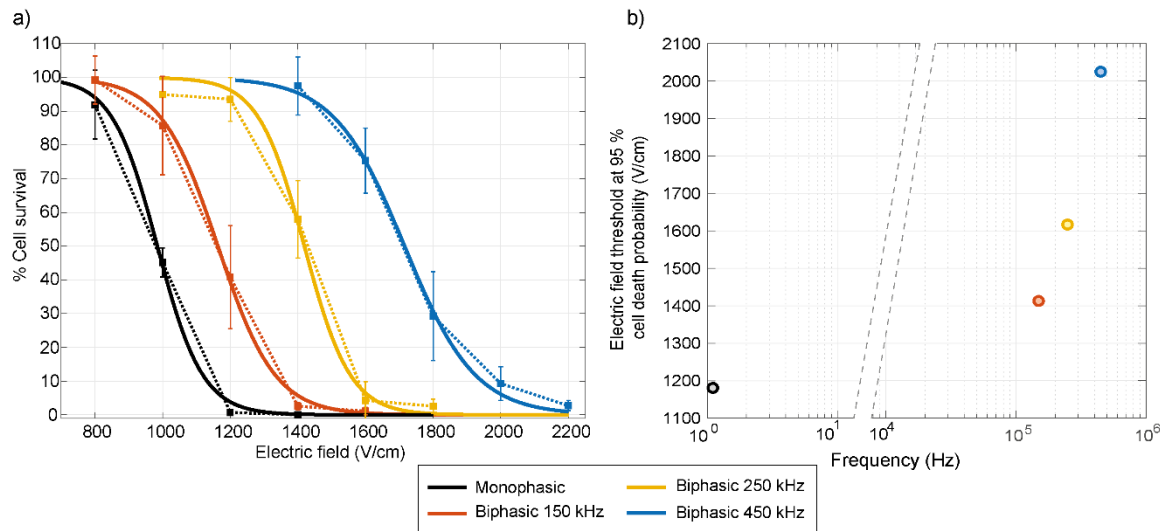


Fig. S1 Results from the in vitro study. a) Cell survival results from the cloning efficacy experiments as a function of EF intensity and the resulting fitted cell death probability models. b) EF magnitude necessary to obtain a 95 % of cell death as a function of the frequency of the applied waveform (values were extracted from the probabilistic models). Note that results from monophasic pulses are placed at very low quasi-DC frequency. For convenience, logarithmic scale of x-axis was broken to improve representation of data.

S.2 Computational model methods

The numerical model simultaneously solved the electric potential, the temperature and the electrical conductivity (σ) distributions in the treatment region during EF application using the coupled physics feature of COMSOL in a time dependent study. The heat source in the system corresponds to the Joule heating produced by the passage of an electric current through a conductor ($\vec{J} \cdot \vec{E}$), where \vec{E} is the electric field and \vec{J} is the current density ($\vec{J} = \sigma \vec{E}$). The conductivity dependence of ionic solutions on temperature variations was also modeled with a linear approximation. Additionally, to account for the EP phenomenon, the conductivity σ of the heart tissue was defined as a sigmoid function of the local EF magnitude, $|\vec{E}|$. Additionally, conductivity of heart tissue also included the contribution of temperature changes.

The conductivity model $\sigma(\vec{E}, T)$ used in the numerical simulations that included contributions of both electric field and temperature was⁵³:

$$\sigma(\vec{E}, T) = \Delta_{\sigma} e^{-e^{-[b(|\vec{E}|-E_0)]}} + \sigma_0(1 + \alpha(T - T_0)) \quad (1)$$

where σ_0 is the initial conductivity of the non-electroporated tissue, Δ_{σ} is the maximum conductivity variation between a non-electroporated and fully-electroporated tissue, b represents the span of the transition zone, E_0 represents the electric field at which conductivity starts to increase due to the electroporation phenomenon, T_0 is the initial temperature (37 °C) and $\alpha=0.015$ stands for the increase of 1.5 % in conductivity increase of ionic solutions per temperature degree.

The values used for σ_0 were extracted from the IFAC-CNR database⁵⁴ for each frequency (monophasic square pulses were approximated to the values at 10 Hz). For parameter b , the value was obtained from data in the literature corresponding to monophasic square pulses and muscle tissue⁵⁵ and was maintained constant for all conditions. As for E_0 , there is no available data in the literature for myocardial tissue in vivo. In fact, most of the recent studies dealing with PFA refer to threshold values extracted from in vitro experiments⁴⁸ that are around 400 V/cm and that may substantially differ from the actual values required in vivo³². Based on that value, in the present simulations we arbitrarily assumed a value of $E_0=500$ V/cm for monophasic 100 μ s pulses. E_0 values for the biphasic pulses at the different frequencies studied were scaled according to the behavior observed in the irreversible electric field threshold obtained in the vitro results presented in this study for CHO cells (refer to next section S2.2). Finally, the values of Δ_{σ} for monophasic pulses were the same values than those used in the literature for muscle tissue⁵⁵. The values of Δ_{σ} for the biphasic pulses at the different frequencies studied were chosen to ensure that the conductivity value of the heart tissue at high electric field intensities (fully electroporated tissue) is similar for all cases.

The blood conductivity dependence on the electric field was not considered in the model because

there is no available data in the literature. Approximating blood behavior to other solid tissues would be highly speculative because only around 50% of blood volume is occupied by cells.

The complete list of values assigned to all parameters and the electrical and thermal properties used in the model can be found in Table TS1. The dependence of electric field intensity on conductivity of heart tissue is plotted for both monophasic pulses and biphasic bursts at the different frequencies simulated in Fig. S2.

Tissue/Material	Condition	Electrical			
		σ_0 (S/m)	Δ_σ (S/m)	b (V/cm) ⁻¹	E_0 (V/cm)
Heart	Monophasic (DC)	$5.37 \cdot 10^{-2}$	0.3	0.01	500
	Biphasic (90 kHz)	0.2119	0.14	0.01	600
	Biphasic (260 kHz)	0.2485	0.105	0.01	900
	Biphasic (450 kHz)	0.2747	0.08	0.01	1300
Blood	Monophasic (DC)	0.7	-	-	-
	Biphasic (90 kHz)	0.7	-	-	-
	Biphasic (260 kHz)	0.71	-	-	-
	Biphasic (450 kHz)	0.74	-	-	-
Electrodes	-	$4.03 \cdot 10^6$	-	-	-

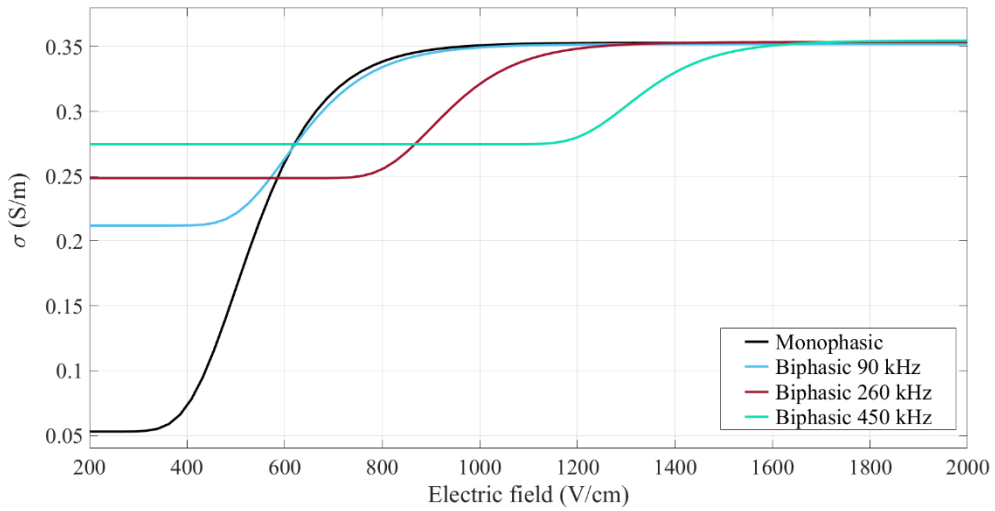


Fig. S2 Modelled conductivity dependence of the heart tissue with the electric field intensity $\sigma(\vec{E})$ for the different waveforms studied.

	Thermal		
	ρ (kg/m ³)	k(W/(m·K))	C_p (J/(kg·K))
Heart	1081	0.56	3686
Blood	1060	0.5	3840
Electrodes	7850	44.5	475

Table TS1 Summary of electrical conductivity and thermal properties used in the computational model for the different tissues/materials. Fig. S2 depicts the conductivity dependence with electric field for the heart tissue at the different frequencies studied.

S.3 Thermal simulations

The computational model was also used to estimate the risk of thermal damage of the experimental electric field delivery protocols. Similar to radiofrequency ablation, the heating source in the present study is due to Joule heating produced by the passage of an electric current through a conductor ($\vec{J} \cdot \vec{E}$). As previously explained conductivity of cardiac tissue was modeled with a double dependence with electric field and temperature $\sigma(\vec{E}, T)$. The numerical model simultaneously solved the electric potential, the temperature and the electrical conductivity distributions in the treatment region during pulse application using the coupled physics feature of COMSOL in a time dependent study. Subsequently, only the temperature dynamics was solved in the period between pulses (1 second). This two-step process was sequentially repeated 10 times (the number of pulses/bursts applied), updating in each step the initial values from the previous iteration. Only heat conduction using the heat transfer in solids equations was modelled. An initial temperature for the tissue and the electrode of 32 °C (corresponding to the temperature measured by the sensor) was considered, the rest of boundaries were fixed at 20 °C.

In Fig. S3 an example of the results obtained from simulations at a biphasic frequency of 90 kHz and the two voltage levels applied (500 and 800) is shown. The temperature evolution is shown at the point of contact between the electrode and the tissue, reproducing the position of the optical temperature probe used in the experiments. As in the real in vivo recordings, the temperature sharply increases during each EP burst (Joule heating) and subsequently slowly dissipates by conduction between consecutive bursts. The maximum absolute temperature variations provided

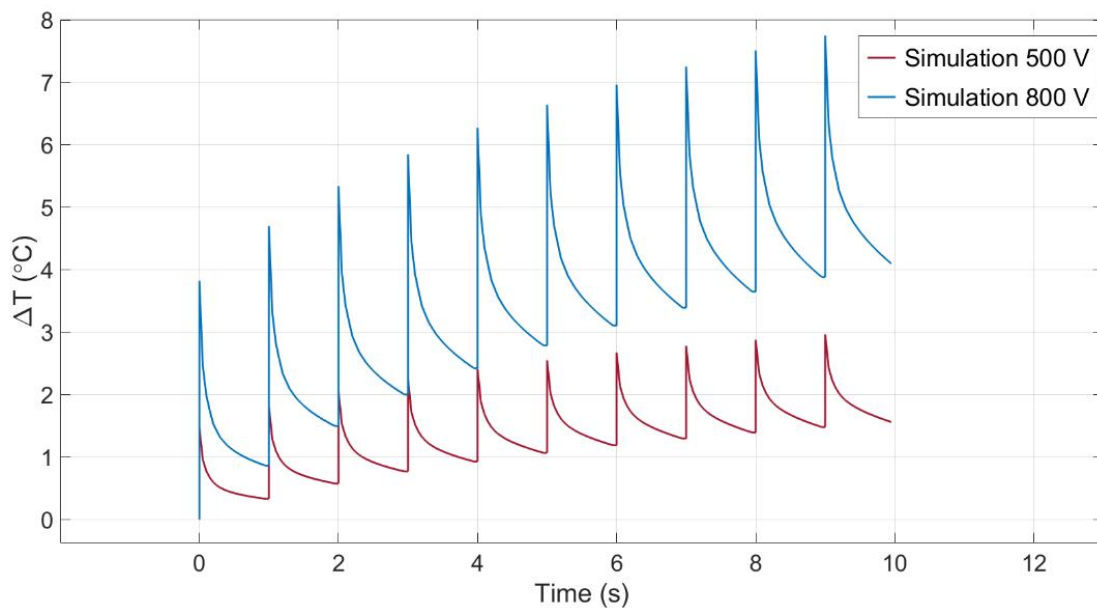


Fig. S3 Results from thermal simulations obtained with a biphasic frequency of 90 kHz and the two voltage levels applied (500 and 800). The temperature variation evolution is shown at the point of contact between the electrode and the tissue for a complete 10-burst sequence.

by the model are significantly higher than the actual measurements performed in vivo (roughly around 3 times higher) but still provide values away from thermal damage.

The deviation between the real measurements and the simulations can be explained by the simplifications assumed in the model. Specially, the heat dissipation effects that the metallic electrode has in the tissue are likely underestimated. Also, actual material properties could differ from the values used in the model (the thermal material properties used are not specific for ventricular epicardium neither specific for the animal model used in the study). More sophisticated modelling strategies could be implemented if the goal was to obtain the most realistic results. However, as the goal of these simulations was to evaluate the risk of thermal damage in a worst case scenario, overestimating the possible heating provides a safety margin that ensures no thermal damage.

S.4 Representative ECG traces

Examples of ECG traces for all conditions are provided in Fig. S4 demonstrating that no significant changes were produced either immediately after or at 3 weeks after treatment. All traces correspond to recordings performed with the chest of the animals closed. Any of the PFA protocols induced ventricular nor supraventricular arrhythmias.

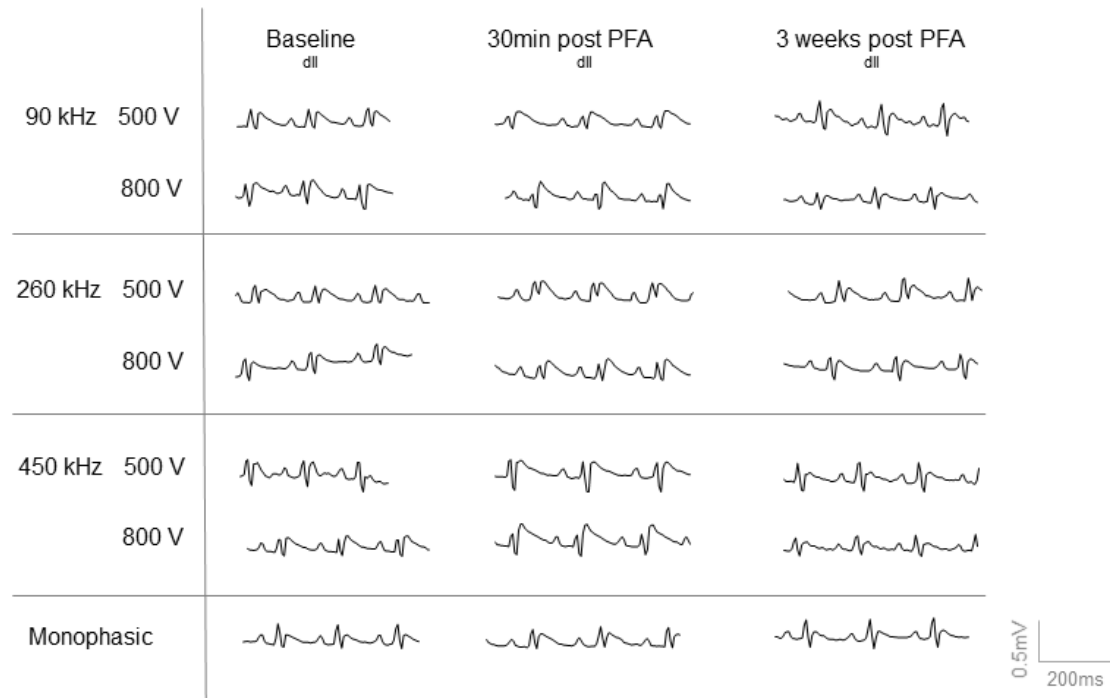


Fig. S4 Representative examples of ECG traces on derivation dII at baseline, 30 min after PFA treatment (thorax already closed) and 3 weeks after PFA treatments.

S.5 Histopathological observations

Observation of the trichrome-stained histological sections by an expert pathologist confirmed fibrosis in the blue-stained areas with preserved structure in arterioles, venules and the rest of medium diameter vessels (see high magnification examples in **¡Error! No se encuentra el origen de la referencia.** lower panels). Lesions displayed homogeneous fibrosis with no evidence of tissue sparing around blood vessels (no effect of blood flow cooling). Signs of perivascular chronic inflammation were observed in some instances at the subepicardial level. In some lesions small surviving cardiomyocytes cores were observed. Most lesions presented relatively well-defined borders with some areas of jagged borders and fibrotic infiltration.

Video legends

Supplementary Video 1. Example of video recording of a complete PFA application corresponding to monophasic pulses at 500 V showing the level of contractions induced.

Supplementary Video 2. Example of video recording of a complete PFA application corresponding to a biphasic waveform of 90 kHz at 500 V showing the level of contractions induced.

Supplementary Video 3. Example of video recording of a complete PFA application corresponding to a biphasic waveform of 260 kHz at 500 V showing the level of contractions induced.

Supplementary Video 4. Example of video recording of a complete PFA application corresponding to a biphasic waveform of 450 kHz at 500 V showing the level of contractions induced.